Role of open volume defects in Mg-doped GaN films studied by positron annihilation spectroscopy

S. Hautakangas and K. Saarinen

Laboratory of Physics, Helsinki University of Technology, P. O. Box 1100, FIN-02150 Espoo, Finland

L. Liszkay*

Institut für Nukleare Festkörperphysik, Universität der Bundeswehr München, 85577 Neubiberg, Germany

J. A. Freitas, Jr. and R. L. Henry

Naval Research Laboratory, Washington, D.C. 20375, USA

We have performed a systematic study by positron annihilation spectroscopy of magnesium-doped, codoped, and annealed GaN films made by metal organic chemical vapor deposition. GaN:Mg films are free of detectable vacancy defects up to $[\mathrm{Mg}] \sim 3 \times 10^{18}$ cm^{-3}, but at doping levels above 10^{19} cm^{-3} vacancies are observed. Two defects are identified: V_{N}-Mg$_{\mathrm{Ga}}$ pairs and vacancy clusters, where the amount of the missing atoms is estimated to be about 60. The defects have an inhomogeneous depth profile with a layer of higher defect concentration starting 100 nm below the surface. Thermal annealing dissociates the V_{N}-Mg$_{\mathrm{Ga}}$ pairs and the vacancy clusters, which migrate and form a homogeneous distribution of smaller clusters through the film. The identified defects play an important role in the electrical compensation and activation of the Mg acceptors in GaN films, and show correlations with results from transmission electron microscopy and photoluminescence studies.

PACS number(s): 78.70.Bj, 72.80.−r, 78.20.−e

I. INTRODUCTION

The *p*-type doping of gallium nitride (GaN) is one of the biggest challenges in GaN-based device development. The *n*-type material is easily achieved by donor impurities doping, e.g., by silicon or oxygen. Presently, the best impurity for *p*-type doping is magnesium, but the room-temperature hole concentrations are generally limited to the moderate level of $\sim 10^{17}$ cm^{-3}.

Hydrogen is always present in epitaxial GaN films grown by metal organic chemical vapor deposition (MOCVD). The H present in the organo metallic precursors can passivate the Mg acceptors in the material. The H can be removed by postgrowth annealing[1] at moderate temperature (~ 800 °C) or by low-energy electron beam irradiation[2] making the material *p*-type conductive. However, there is experimental evidence that a nitrogen vacancy (V_{N}) can be a compensating center for the Mg acceptor.[3,4] The calculated formation energies of V_{N} and Mg$_{\mathrm{Ga}}$-V_{N} pairs are low[5] in *p*-type material. The activation energy for V_{N} diffusion is controlled by Fermi level E_F.[6] When E_F is in the midgap the charge state of V_{N} is +1 and the diffusion is unlikely to happen. In *p*-type GaN the N vacancy has a charge state +3 which is much more mobile.

Great effort has been put into studies of large open volume defects like vacancy clusters and pinholes in Mg-doped GaN. Liliental-Weber *et al.* have shown with transmission electron microscopy measurements that Mg dopants segregate in the planar defects.[7] These Mg atoms are likely to be electrically inactive. They have also shown that the Mg decoration of the hollow pyramidal defects correlates with the change of crystal polarity during growth.[8]

We use positron annihilation spectroscopy to investigate the native defects in Mg-doped GaN films. The method is an effective tool for studying vacancy-type defects in semiconductors (see, e.g., Ref. 9). Because of the positron charge, it can be found in the region where the positive background is reduced. The positron is trapped by negative and neutral vacancies due to the missing positive ion core. The trapping increases the lifetime of the positron and narrows the momentum distribution of the positron-electron pair. These annihilation data can be used to distinguish between different vacancy-related defect types as well as to estimate the vacancy concentration with sensitivity in the range 10^{16}–10^{19} cm^{-3}. The momentum distribution of the electron at the vacancy can be measured directly in the energy distribution of the annihilation photons. This enables the identification of atoms neighboring the vacancy.

In our previous publication[10] we have shown that nitrogen vacancy is a compensating center in Mg-doped GaN. The N vacancy can be removed by annealing at moderate temperature. The vacancy was identified as a neutral Mg$_{\mathrm{Ga}}$-V_{N} pair, which dissociates by thermal annealing, leading to a diffusing nitrogen vacancy. In this paper we investigate further the nature of vacancy-related defects in Mg-doped, codoped, and thermally annealed GaN films. In addition to nitrogen vacancy complexes, we also focus on larger vacancy clusters, which have been previously observed in Mg-doped GaN.[10,11] These defects may also have influence on the compensation level of the material.

In Sec. II we describe the experimental setup and samples used in this study and in Sec. III we present our results obtained with positron annihilation measurements. In Sec. IV we discuss the mechanism of electrical compensation as well as the effect of annealing and compare these results with those obtained by other measurement methods. A summary of our results is given in Sec. V.

TABLE I. The Mg and Si concentrations measured by secondary-ion mass spectrometry in studied GaN layers. The hole concentrations were determined by Hall measurement (Ref. 12) and in the case of reference sample (Ref. 13) with capacitance-voltage measurements. RTA stands for rapid thermal annealing and SITU means that samples were annealed in the growth reactor. The GaN:Mg reference is the same sample as studied in Ref. 13.

Sample number	Mg concentration (10^{19} cm^{-3})	Si concentration (10^{17} cm^{-3})	Hole concentration (10^{17} cm^{-3})	Annealing temperature (°C)
1	4.0	1.3	highly resistive	No anneal.
2	4.0	1.3	1.7	980/RTA
3	7.3	72	highly resistive	No anneal.
4	9.0	84		1000/RTA
5	1-2	5-6	highly resistive	800/SITU
6	0.25	5-6	highly resistive	800/SITU
GaN:Mg reference			~10	No anneal.

II. EXPERIMENTAL DETAILS AND SAMPLES

A. Samples

The experiments were performed on six epitaxial GaN films, referred to as Nos. 1–6, grown on *a*-plane sapphire substrates by MOCVD. Secondary-ion mass spectrometry was employed to determine the total Mg, Si, H, O, and C concentrations in the films. The magnesium concentration of samples varies in the range $(0.25–9) \times 10^{19}$ cm^{-3} and $[Si] = (0.13–8.4) \times 10^{18}$ cm^{-3}. In addition, sample 2 has hydrogen concentration of 4×10^{18} cm^{-3} and $[O] = 1 \times 10^{17}$ cm^{-3}. Samples 3 and 4 are intentionally codoped with Si; the other samples have moderate Si concentration coming from the reactor walls during growth. Note that the samples 2 and 6 are the same as studied in Ref. 12 (samples 4 and 1 therein). The postgrowth heat treatments were done by rapid thermal annealing (RTA) at 980 °C and in the case of Si codoping at 1000 °C. As can be seen in Table I the Mg concentration is over two orders of magnitude bigger than the hole concentration in sample 2. A *p*-type Mg-doped GaN sample grown by molecular beam epitaxy (MBE) was used as a vacancy-free reference sample.[13]

The photoluminescence (PL) experiments were carried out at 6 K; the PL was excited by the 325 nm line of a HeCd laser at a power density of ~8 W/cm^2. The light emitted by the samples was dispersed by a double-grating spectrometer fitted with 1800 groves/mm. A uv-extended GaAs photomultiplier coupled to a computer-controlled photon counter was used for data acquisition. The PL spectra were corrected for the instrumental response by normalization to the throughput of a broadband calibrated lamp. To illustrate the optoelectronic properties of Mg-doped samples we represent in Fig. 1 the PL spectra of three GaN films (indicated as *S#a*, *S#b*, and *S#c*) doped with increasing concentration of Mg. The relative redshift of the peak positions with increasing doping level has been attributed to potential fluctuation induced by charged donor or acceptor centers and to the incorporation of deep donors, respectively.[14,15]

B. Positron Doppler spectroscopy

After implantation into the material the positron loses its energy and reaches a thermal equilibrium with its surround-

ings in a few picoseconds and starts to diffuse. Negatively charged and neutral defects, especially vacancies, can trap the positron. Finally, the positron annihilates with an electron into two 511 keV γ quanta. The 511 keV annihilation line is broadened because of the momentum of the electron. By studying the Doppler shift of the annihilation energy the information about the electron configuration at the annihilation site can be revealed.

The energy distribution of annihilated positron-electron pairs is characterized by the S and W parameters (see, e.g., Ref. 16). The S parameter measures counts of the central part of the 511 keV peak and the W parameter describes the counts in the wing areas of the peak. Thus the S parameter represents annihilations with valence electrons with longitudinal momentum component of $p_L \lesssim 3.7 \times 10^{-3} m_0 c$ and the W parameter describes the annihilations with high-momentum core electrons, $11 \times 10^{-3} m_0 c \lesssim p_L \lesssim 29 \times 10^{-3} m_0 c$. At a vacancy the electron momentum is locally decreased, which leads to narrowing of the energy distribution of annihilation photons. This can be characterized as a higher S parameter and a lower W parameter than in the bulk material.

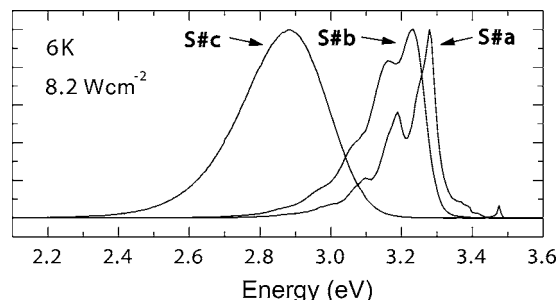The valence annihilation parameter S is a linear superposition of the values S_i

FIG. 1. Normalized low-temperature PL spectra of three GaN:Mg epitaxial films deposited by MOCVD on *a*-face sapphire substrates. Note the line shape change and the redshift of the peak position with increasing Mg concentration, from 2.5×10^{18} to 7×10^{19} cm^{-3}. These samples have been postgrowth thermally annealed at 950 °C. The spectra are corrected for instrumental response.

$$S = \eta_b S_b + \sum_{i=1}^{N} \eta_i S_i, \qquad (1)$$

where S_i and S_b are the characteristic S parameter values for annihilations in different positron states, and weighting factors η_i and η_b are the fractions of positron annihilations at each state. The letter b denotes the annihilations of delocalized positrons. A similar equation holds for the W parameter. If only one vacancy-type defect trapped the positron, the experimental S and W parameters would be linear combinations of the values (S_b, W_b) and (S_V, W_V), which correspond to annihilations of the free positron in the defect-free lattice and annihilations of positron trapped at vacancies, respectively. The measured S and W parameters would then fall on a line connecting the points (S_b, W_b) and (S_V, W_V) in the S-W plot. This analysis enables one to distinguish between different annihilation sites.

We use a low-energy positron beam. The positrons emitted from the ^{22}Na source with initial energies up to several hundred keV are moderated using W foil. After moderation positrons are accelerated to energies between 0 and 30 keV. The annihilation radiation is detected with high-resolution (1.2 keV at 511 keV) germanium detectors.

C. Positron lifetime spectroscopy

The trapping of positrons at the vacancy increases the average lifetime of the positron because the electron density is reduced at the vacancy. By measuring the lifetime one can distinguish between different open volume defects and estimate their concentrations. A pulsed low-energy positron beam enables lifetime measurements in thin semiconductor layers. The positron lifetime is measured as the time interval between an annihilation γ photon and the beam pulse edge, where the pulsing is done after positron moderation. About 2×10^6 counts are measured for the peak to have reliable information about the defects in the samples.

To find the average lifetimes and to decompose the lifetime spectra the resolution has to be taken into account. After subtracting the background the lifetime spectra can be analyzed as a sum of exponential decay components $n(t) = \Sigma_i I_i \exp(-\lambda_i t)$. The resolution function is a sum of three Gaussian distributions. The center of mass of the lifetime spectrum $\tau_{av} = \Sigma_i I_i \tau_i$ increases with increased positron trapping into vacancies.

III. POSITRON STUDIES

A. Doppler results

Figure 2 shows the S parameter as a function of incident positron energy in samples with different Mg concentrations. The reference level corresponding to the vacancy-free lattice is represented by the dashed line. In the lattice, the positron wave function is delocalized. The annihilation from a bulk state gives the most broadened momentum distribution, which can be seen as a low S parameter. The vacancy-free S parameter level as well as the bulk lifetime ($\tau_b = 160 \pm 5$ ps) in GaN are well known on the basis of previous studies.[10]
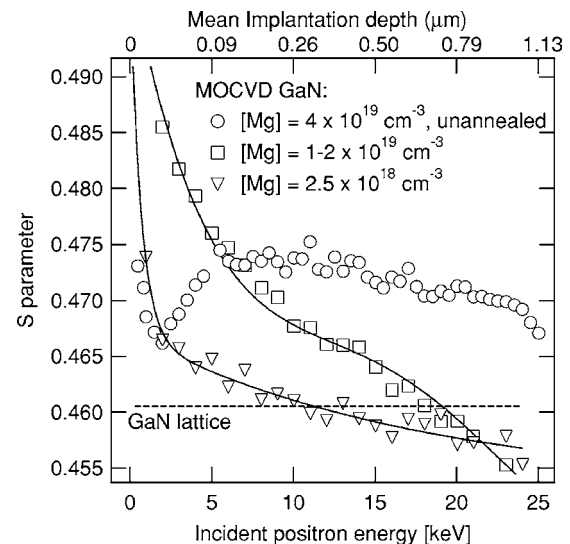

FIG. 2. The valence annihilation parameter S as a function of incident positron energy in GaN layers. The samples were annealed at 800 °C except the one with highest Mg concentration. The dashed line represents the S parameter level of annihilations of delocalized positrons in the GaN lattice. The top axis indicates the mean implantation depth of the incident positron. The solid lines are to guide the eye.

Here we use a MBE-grown GaN:Mg reference sample, which has the same positron lifetime as a defect-free GaN lattice according to earlier measurements.[10,13,17]

In Fig. 2 the top axis shows the mean implantation depth of a positron related to the acceleration voltage used. The behavior of the S parameter can be divided into three different regions: (1) surface, (2) layer, and (3) substrate. At low acceleration energy (<2 keV) the penetration depth of positrons is low and they can diffuse back to the surface. The electron density is reduced at the surface, resulting in a narrower annihilation line, which is observed as a higher S parameter. At higher acceleration voltage ($5-20$ keV) the S parameter characterizes the GaN layer. At even higher energies the S parameter is decreasing because the positrons are implanted in the sapphire substrate, where the electron momentum is higher. The measured S parameter is hence a linear combination of the individual S parameters of each region with corresponding weighting factors η_i [see Eq. (1)].

To study the effect of Mg doping one has to focus in the region of 250–500 nm (Fig. 2). The sample containing the lowest Mg concentration has the same S parameter level as in bulk GaN. No vacancies are thus detected. On the other hand, the S parameter is ~ 0.466 for the sample with Mg concentration of $(1-2) \times 10^{19}$ cm^{-3}, and $S \sim 0.473$ for sample 1 with the highest Mg concentration. As can be seen the S parameter levels of samples have a clear order depending on the Mg content. A higher S parameter value is a fingerprint of a vacancy-type defect. At the vacancy the electron density is decreased and the annihilation line is narrower, yielding a higher S parameter than in the bulk lattice. Hence, positrons reveal increased trapping in vacancy-type defects with higher Mg concentrations.

GaN:Mg samples are often used as vacancy-free reference samples because even if vacancies exist, they are likely to be
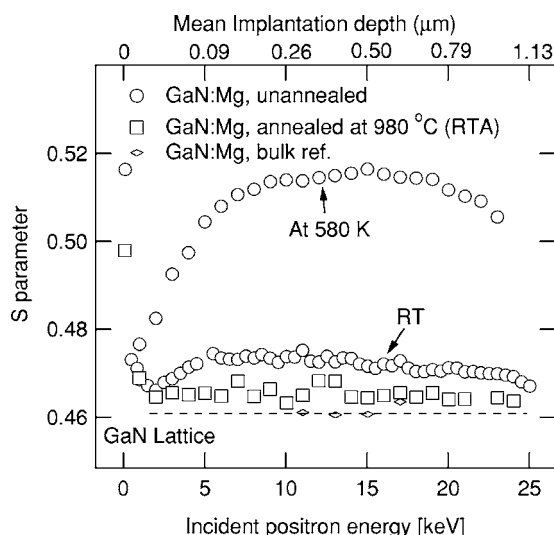
FIG. 3. The valence annihilation parameter S as a function of incident positron energy in annealed and unannealed GaN:Mg samples with Mg concentration of 4×10^{19} cm^{-3}. p-type GaN:Mg is used as a vacancy-free reference. The top axis indicates the mean penetration depth.

FIG. 4. Valence annihilation parameter S as a function of measuring temperature. The incident positron energy was chosen high enough to make sure the annihilations arising from the surface are excluded.

in the positive charge state and hence cannot trap positrons. The data of Fig. 2 indicate, however, that at very high Mg concentrations vacancy-related defects acting as positron traps are created.

Figure 3 shows the low-momentum parameter S as a function of incident positron energy at room temperature for both unannealed and annealed GaN:Mg with Mg concentration of 4×10^{19} cm^{-3} and for the reference sample. The S parameter for unannealed sample 1 measured at 580 K is also represented. At low positron acceleration energies (0–2 keV) the S parameter of all samples is high due to the annihilation at surface states and decreases with increasing positron energies. Deeper probing (50–260 nm) of the unannealed GaN:Mg sample shows that the S parameter increases and reaches a plateau with constant value $S \approx 0.473$ at 300 K and $S \approx 0.515$ at 580 K, in the depth range between 260 and 790 nm. Excluding the surface, the S parameter of the annealed sample has a constant value $S \approx 0.465$. At positron energies above 20 keV the S parameter starts to decrease due to annihilations at the Al$_2$O$_3$ substrate.

S parameter values higher than the bulk level indicate the presence of vacancy-type defects (Fig. 3). It is evident from the experiment that a high measuring temperature makes trapping at vacancies more effective. Right below the surface the S parameter of the unannealed sample has a local minimum, which corresponds to a region with lower vacancy concentration. After annealing the vacancy signal is still evident, but the profile is homogeneous. Comparing Figs. 2 and 3 one can deduce that high Mg content generates a vacancy profile where the lower vacancy concentration is below the surface and it increases deeper in the layer.

The temperature behavior of the valence annihilation parameter S is shown in Fig. 4. The S parameter level for the vacancy-free p-type reference sample is indicated with a dashed line. At high temperatures (>300 K) the S parameters of samples 1 and 2 are clearly higher than that of the
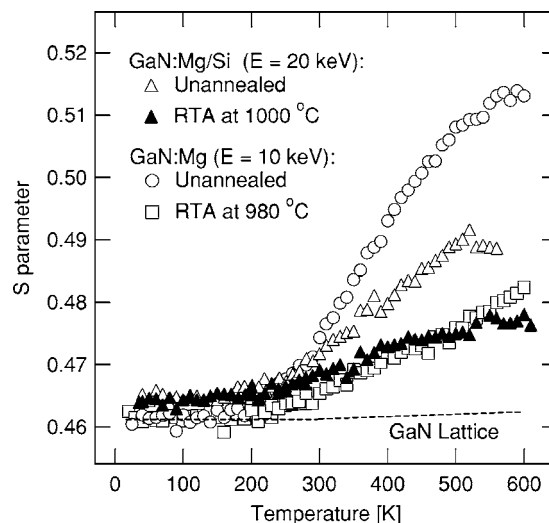
reference sample. At 600 K the S parameter of the unannealed GaN:Mg sample reaches a value of $S \approx 0.513$ and the value of the annealed sample increases up to $S \approx 0.481$. The S parameters of codoped samples are also higher than that of the reference sample, indicating positron trapping at the vacancies.

In addition to vacancies, positrons trapped by negative ions can also be detected in the data of Fig. 4. At low temperatures the S parameter approaches the lattice value, indicating fewer annihilations at vacancies. This behavior is typical when negative ions trap positrons at weakly localized states (binding energy 10–100 meV). The electron density around the negative ion is almost the same as in the bulk lattice, leading to a similar S parameter and positron lifetime values. Such shallow positron traps have been observed in GaN also before, and they have been attributed to Mg$_{Ga}$ acceptors[18] and dislocations.[19]

B. Lifetime results

Figure 5 shows the average positron lifetime τ_{av} as a function of incident positron energy in the unannealed GaN:Mg sample measured at 300 K. At the surface the average lifetime is high due to the low electron density. The average lifetime is lowest with positron energy of 2 keV and increases to the constant value of $\tau_{av} = 185$ ps in the range of 100–500 nm. When probing deeper in the sample, τ_{av} decreases due to the annihilations in the sapphire substrate. As can be seen in Fig. 5 there is a region of lower vacancy concentration below the surface in agreement with the result obtained by Doppler measurement (Fig. 3).

The average lifetime of a positron as a function of temperature is shown in Fig. 6. At low temperature ($T = 85$ K) $\tau_{av} \approx 150$ ps is equal to the lifetime of the defect-free lattice, similarly as seen in the Doppler experiment in Fig. 4. Therefore, positrons are trapped at shallow traps (negative ions,
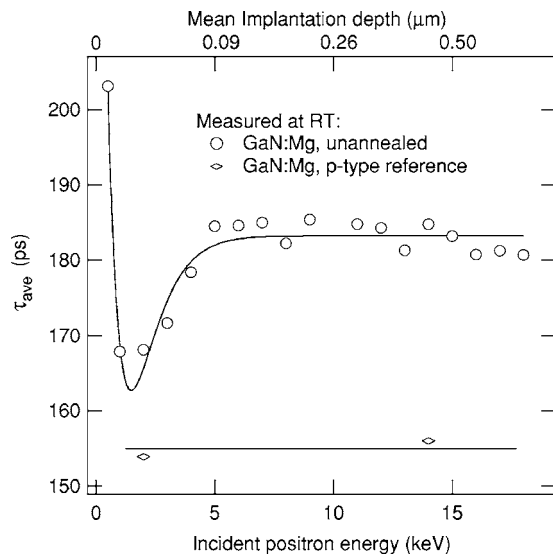
FIG. 5. The average lifetime of positrons as a function of incident positron energy in the unannealed GaN:Mg sample. A p-type Ga:Mg sample is used as a vacancy-free reference. The solid line is to guide the eye.

dislocations) preventing annihilation at vacancies. With increasing temperature the average lifetime increases up to 223 ps because positrons escape from the shallow trap and a larger fraction of them annihilate at vacancies.

C. Identification of vacancies

To analyze the annihilation parameters independently of the vacancy concentration the core annihilation parameter W can be shown as a function of valence annihilation parameter S. Figure 7 shows the W vs S plot measured in the annealed and unannealed samples. Both of these parameters were normalized with those measured for the GaN lattice. The slope of the S-W plot characterizes the defect species and does not
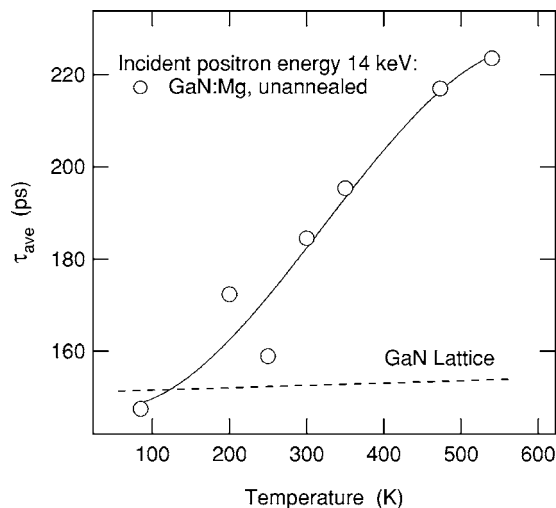

FIG. 6. The average positron lifetime of an unannealed GaN:Mg sample as a function of measuring temperature. The incident positron energy was 14 keV. The solid line is to guide the eye.
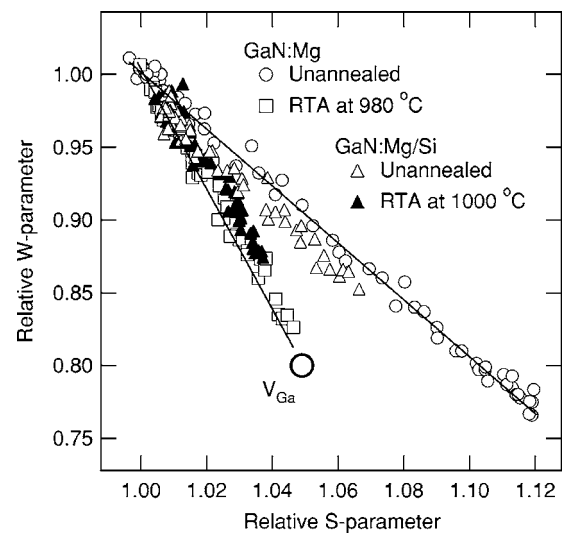

FIG. 7. The core annihilation parameter W as a function of valence annihilation parameter S measured at different temperatures. V_{Ga} represents the positron annihilation parameters at a Ga vacancy. Note that the data are the same as in Fig. 4.

depend on the concentration of the vacancy (see Sec. II B).

Figure 7 also shows the characteristic S and W parameters for a gallium vacancy (V_{Ga}) as obtained in Ref. 20. The slope of the S-W plot for the as-grown sample 1 is almost the same as measured before[21] for a vacancy cluster. Furthermore, the slope of the S-W plot is constant, which means that a single vacancy defect type dominates the Doppler-broadened spectrum. The change in relative S parameter ($S/S_b \sim 1.1$) of the unannealed sample is typical for vacancy clusters and much larger than expected for monovacancies.

After annealing, the change in the relative S parameter is more moderate ($S/S_b \sim 1.045$). This S parameter is close to those determined for the native Ga vacancy.[20] Again the slope is constant, indicating a single dominant vacancy defect type. However, the slope differs from the one before annealing, which shows that the dominant type of vacancy defect changes. Since the (S,W) parameter become closer to that of V_{Ga}, we conclude that the size of the vacancy cluster decreases with thermal annealing.

The codoping of GaN:Mg samples with Si atoms generates also vacancy-related defects as observed in Fig. 4. Before annealing they have a characteristic slope in the S-W plot (Fig. 7) revealing the existence of vacancy clusters. We conclude that the annealing changes the slope, similarly as in the Mg-doped samples 1 and 2. The annealing makes these clusters convert to vacancy defects with smaller size, with annihilation parameters close to those of V_{Ga}.

To identify vacancies and to study their profile in the GaN:Mg sample 1 (see Figs. 2, 3, and 5) a positron lifetime measurement with two different acceleration voltages has been performed (Fig. 8). The measurement voltages were 2 and 14 keV where maximum effects in the depth profile can be expected (Figs. 3 and 5). Figure 8 also shows the lifetime spectrum of a MBE-grown GaN:Mg reference sample, which was measured at 300 K using acceleration voltage of 14 keV to minimize annihilation events at the surface. Only one life-
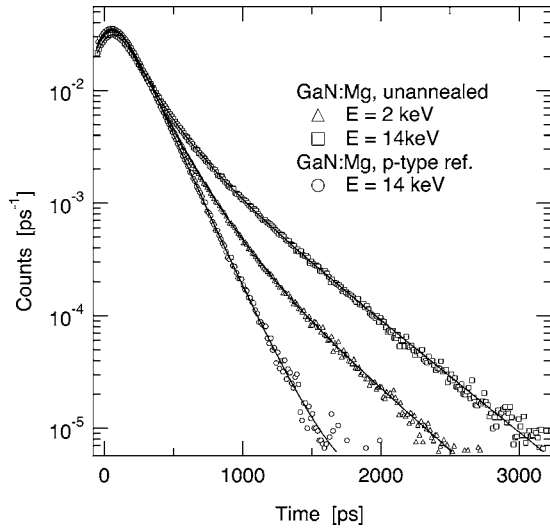
FIG. 8. Positron lifetime spectra in the unannealed GaN:Mg sample measured with two different positron energies at 540 K. A Mg-doped MBE-grown *p*-type sample is shown as a vacancy-free reference. The area of each spectrum was scaled to 1. Solid lines are the fitting results of the respective spectra.

time component can be distinguished from the spectrum of the reference sample with the value of $\tau_{\text{bulk}} = 155 \pm 1$ ps. This is consistent with theoretical calculations,[22] where $\tau_{\text{bulk}} = 156$ ps, and it is similar to previously measured values for positron annihilation in the GaN lattice.[10,17]

The decompositions of the lifetime spectra are shown in Table II. In the unannealed sample 1 three different lifetimes components are found. The smallest is $\tau_1 \approx 70$ ps which is related to positron annihilations in the delocalized state. In the presence of open volume defects the lowest lifetime is clearly smaller than the bulk lifetime. This happens because of the trapping: The free positron annihilation has to take place before trapping into the vacancy.

The spectrum of unannealed GaN:Mg measured at 14 keV (Fig. 8) reveals high intensities of two vacancy-related lifetimes. The lower is $\tau_2 = 180$ ps and the higher is $\tau_2 = 435$ ps, which are close to values detected previously.[10] The shorter lifetime $\tau_2 = 180$ ps is clearly longer than the lifetime in the GaN lattice. On the other hand it is shorter than that obtained for a gallium vacancy $\tau_{V_{\text{Ga}}} = 235 \pm 5$ ps.[20] The natural identification is then the nitrogen vacancy. The isolated V_{N} is positive and cannot trap positrons, so the V_{N} has to be neutralized with an impurity, namely, with the Mg

atom.[10] The formation energy of the V_{N}-Mg_{Ga} complex is calculated to be small in *p*-type material.[5,6] The lifetime τ_2 is the same as reported previously,[10] where $\tau_2 = 180$ ps is connected to the V_{N}-Mg_{Ga} complex by studying the chemical environment of the vacancy with a Doppler broadening measurement. The electron configuration at the site of V_{N} is different depending on the neighborhood of the vacancy. The replacement of the Ga atom by a Mg atom was verified by reduced counts in the high-momentum part of the annihilation energy.[10] Mg does not have $3d$ electrons with high momenta. We thus attribute the lifetime component of 180 ps to positron annihilation at the V_{N}-Mg_{Ga} complex.

The longer-lifetime component $\tau_3 = 435$ ps is so large that it cannot arise from single monovacancies. The lifetime of 435 ps is hence attributed to a vacancy cluster. The size of the vacancy cluster is discussed in more detail below.

Interestingly the Doppler measurement and the (S, W) plot reveals only one vacancy-type defect in the unannealed GaN:Mg, namely, vacancy clusters, whereas the decomposition of the lifetime spectra of the same sample yields two vacancy-related lifetimes. We think that this behavior is related to the sensitivity of the S vs W plot. Since the S and W parameters are dominated by the annihilations at the vacancy cluster, the V_{N}-Mg_{Ga} complex is not revealed in the (S, W) plot since its momentum distribution is almost the same as in the bulk lattice.

In summary, positrons reveal two vacancy defects in as-grown unannealed GaN:Mg: (i) the V_{N}-Mg_{Ga} complex and (ii) the vacancy cluster. The concentration of V_{N}-Mg_{Ga} complexes increases with increasing Mg concentration and cluster formation is observed only for Mg doping levels of $\geq 10^{19}$ cm^{-3}. After thermal annealing, vacancies are still detected, but their open volume is smaller and their annihilation parameters are close to those of V_{Ga}. We attribute these to smaller vacancy clusters which are formed by dissociation of the larger vacancy clusters during the thermal annealing process.

D. Vacancy cluster size and saturation lifetime

It has been shown that the positron lifetime at vacancy clusters is sensitive to the size of the clusters.[23,24] To estimate the size of the open volume with the positron lifetime of 435 ps we calculate the positron lifetimes theoretically. For the positron states we use the conventional scheme with the local density approximation (LDA) for electron-positron correlation effects and the atomic superposition method in the

TABLE II. Decomposed lifetimes of the unannealed GaN:Mg sample measured at two different positron energies. Background reduction was 0.3% 500 ps at 14 keV and 5–6 % 350 ps extra component at 2 keV. The latter arises from surface annihilations and is hence dependent on the measuring temperature. The defect concentrations are determined from the decomposed lifetimes by applying the positron trapping model [Eqs. (4)–(6)].

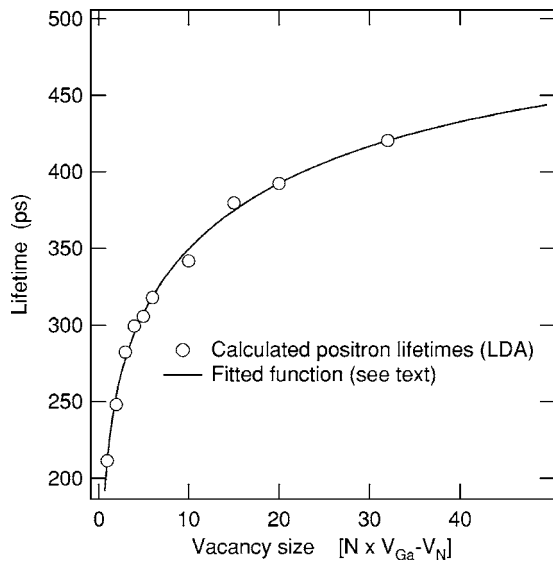| Sample	Positron energy (keV)	Temperature (K)	τ_{av} $(10^{-9}$ s)	τ_1/I_1 (ps/%)	τ_2/I_2 (ps/%)	τ_3/I_3 (ps/%)	Vacancy concentration $(10^{17}$ cm$^{-3})$	Cluster concentration $(10^{15}$ cm$^{-3})$
Unannealed	14	540	223(1)	70(2)/27(1)	183(3)/45(1)	435(3)/28(1)	2.7	4.5
	2	540	159(1)	71(4)/27(2)	173(3)/68(2)	438(9)/5(1)	1.9	0.5

FIG. 9. The calculated positron lifetime as a function of the number of vacancy pairs. The solid line is a fit of a function where the electron density n is scaled to the vacancy cluster size [Eq. (3)].

numerical calculations.[25,26] The positron annihilation rate λ is

$$\tau^{-1} = \lambda = \pi r_0^2 c \int d\boldsymbol{r} |\psi_+(\boldsymbol{r})|^2 n_-(\boldsymbol{r}) \gamma[n_-(\boldsymbol{r})], \qquad (2)$$

where n_- is the electron density, $\psi_+(\boldsymbol{r})$ the positron wave function, r_0 the classical electron radius, c the speed of light, and γ the enhancement factor, for which we use the interpolation by Boronski and Nieminen.[27] The positron state was solved in a 216-atom supercell, in vacancy clusters up to the size of 62 missing atoms (Fig. 9).

As can be seen in Fig. 9 the positron lifetime starts to saturate above 400 ps when the cluster includes more than 30 V_{Ga}-V_N vacancy pairs. This is the consequence of the reduced electron density at the annihilation site. The solid line in Fig. 9 represents the annihilation rate

$$\lambda = \tau^{-1} = (2 + Ae^{-BN^{1/3}} + Ce^{-DN^{1/3}}) \times 10^9 \text{ s}^{-1}, \qquad (3)$$

where N is the vacancy size and A–D are fitting parameters with values of 53.05, 4.57, 4.89, and 0.81, respectively. The function has a saturation lifetime 500 ps, which is the lifetime of the negative positronium atom, similarly as in the Brandt-Reinheimer formula.[26,28]

The electron density n in a vacancy cluster plays a crucial role when determining the annihilation rate of a positron. We motivate Eq. (3) in the following way. The gallium atom is much bigger than nitrogen, and the positron probes mainly the electron density of a Ga atom. The electron density of a Ga atom decreases exponentially ($n \propto e^{-r}$) with the radial distance $r \propto N^{1/3}$. At small cluster sizes positrons annihilate with both Ga ($4s$, $4p$) valence electrons and Ga ($3d$) core electrons. In larger vacancy clusters the annihilation with the valence electrons strongly dominates. Hence, the fitted sum of two exponential functions can be thought of as annihilations with two different electron shells, which is controlled

by the size of the vacancy cluster N. As seen in Fig. 9, the simple scaling of Eq. (3) reproduces very well the positron lifetimes calculated with the atomic superposition method [Eq. (2)]. The result of Fig. 9 is quantitatively similar to the behavior of the calculated positron lifetime in Fe vacancy clusters.[29] This means that the number of missing Ga atoms determines the positron lifetime.

The experimental positron lifetime of 435 ps is close to the saturation value of the curve represented in Fig. 9, but yet smaller than the $n \rightarrow 0$ limit of 500 ps of the Brandt-Reinheimer formula.[26,28] The theoretical limit value of 500 ps has been experimentally observed in other GaN:Mg samples,[10] as well as in deformed Si (Ref. 30) or GaAs.[29] These comparisons suggest that the lifetime of 435 ps has not yet reached the saturation regime as a function of the vacancy cluster size. Therefore, we attribute it to clusters where about 60 atoms (30 GaN molecules) are missing (cluster radius of ~5 Å).

E. Vacancy concentrations

The positron trapping into the vacancies depends on the measuring temperature and the vacancy charge state.[31] Positive vacancies cannot trap positron due to Coulombic repulsion. Neutral and negative vacancies can trap positrons with the trapping rate

$$\kappa = \mu c, \qquad (4)$$

where μ and c are the trapping coefficient and the defect concentration, respectively. In the case of large vacancy clusters the trapping is limited by positron diffusion and the trapping rate is

$$\kappa = 4\pi r D_+ c, \qquad (5)$$

where r is the radius of the void and D_+ is the diffusion constant of the positron.

The vacancy concentrations can be calculated from the trapping rate κ. On the basis of the intensities of the lifetime components one can deduce κ_V and κ_{cl}. The concentrations are calculated from the equations $[V_N\text{-}Mg_{Ga}] = N_{at}\kappa_V/\mu_V$ and $[V_{cl}] = N_{at}\kappa_{cl}/\mu_{cl}$ for vacancy- and cluster-type defects, respectively. $N_{at} = 8.78 \times 10^{22}$ cm^{-3} is the atomic density of the material and $\mu_V = 10^{15}$ s^{-1} is the trapping coefficient for the transition-limited trapping, i.e., for monovacancies. In the case of vacancy cluster the size is $r = 5$ Å (estimated above) and $D_+ = 1$ cm^2/s giving $\mu_{cl} = 4\pi r D_+ N_{at} = 5.5 \times 10^{16}$ s^{-1}.

The model applied here includes two different types of vacancy defects and no detrapping, i.e., no positrons escaping from the trap. This is reasonable because the measuring temperature is 540 K and the thermal energy is high enough to prevent trapping at shallow traps, i.e., negative ions or dislocations. All different positron states were considered to be noninteracting. The trapping rates κ_V and κ_{cl} can be calculated with the help of intensities I_2 and I_3 from the positron lifetime measurement

$$I_2 = \frac{\kappa_V}{\lambda_b - \lambda_V + \kappa_V + \kappa_{cl}},$$

$$I_3 = \frac{\kappa_{cl}}{\lambda_b - \lambda_{cl} + \kappa_V + \kappa_{cl}}, \tag{6}$$

where $\lambda_b = \tau_b^{-1} = (155 \text{ ps})^{-1}$, $\lambda_V = \tau_V^{-1} = (180 \text{ ps})^{-1}$, and $\lambda_{cl} = \tau_{cl}^{-1} = (435 \text{ ps})^{-1}$. I_2 and I_3 are the intensities of τ_2 and τ_3, respectively, and they are listed in Table II. As can be seen from Table II the vacancy as well as the cluster concentrations are lower near the surface. The decrease in V_N-Mg_{Ga} concentration is small while the cluster concentration is an order of magnitude smaller close to the surface. The inhomogeneous vacancy concentration, observed both in the S parameter and in the average positron lifetime, evidently arises from the vacancy cluster concentration.

IV. DISCUSSION

A. Mg doping, electrical compensation, and vacancy defects

The electrical inactivity of Mg acceptors in GaN:Mg is generally associated with the passivation induced by hydrogen atoms. MOCVD growth uses Ga atom precursors in the form of trimethylenegallium and the residual H in the growth environment is readily available to passivate the Mg acceptor. The migration barrier for H is low, and annealing at moderate temperatures activates the Mg acceptors by dissociating the H from the Mg atoms. The binding of hydrogen to Mg ions and its dissociation have been observed by local vibrational mode spectroscopy[32,33] and the results are generally in agreement with theoretical calculations.[34]

The high level of Mg doping (above 10^{19} cm^{-3}) seems to cause competing mechanisms for Mg deactivation. The V_N-Mg_{Ga} pairs observed here by positron spectroscopy compensate Mg atoms making the material more resistive. The postgrowth annealing decreases the concentration of V_N-Mg_{Ga} complexes, which can be interpreted as the dissociation of the V_N-Mg_{Ga} pairs.[10] This process leads to electrically active Mg ions, in an analogous manner as in the case of H passivation. Furthermore, the vacancy clusters observed here may also have a role in the electrical compensation of Mg doping.

Liliental-Weber *et al.* have studied the formation of pyramidal defects in Mg-doped GaN. These defects are associated with inversion domains,[8,35] and according to tranmission electron microscope (TEM) measurement they are hollow. The defects are further decorated by Mg,[7,36] which suggests that they are important for the compensation of the material. Comparing this with the present positron studies, we can conclude that the high S parameter value as well as the high intensity of the long-positron-lifetime component correlate well with the TEM results. In addition, the inhomogeneous cluster profile is in good agreement with the typical TEM images,[37] suggesting strongly that the profile of the open volume (detected by positrons) corresponds to that of the pyramidal defects. On the other hand, the size of the vacancy clusters detected here (60 atoms, 0.5 nm radius) is smaller than the typical size of the pyramidal defects observed by TEM (1–10 nm). The positron spectroscopy is perhaps sensitive primarily to smaller vacancy clusters than those reported by TEM experiments, although the origin of

both observations could be similar, i.e., the inversion domain triggered by Mg doping.

The positron annihilation data allow one to estimate quantitatively the Mg compensation by vacancy defects. The concentration of passivated Mg acceptors can be estimated by taking the value[38] of $1.25m_e$ for the effective hole mass in GaN and 0.2 eV for the ionization energy E_a for the acceptors. By simple Fermi statistics[38] one can find the level of ionized Mg to be 3.3×10^{18} cm^{-3} without compensating defects.[39] The concentration of V_N-Mg_{Ga} complexes is $(2-3) \times 10^{17}$ cm^{-3} according to the analysis of the positron data (Table II). This defect thus contributes to the electrical deactivation of Mg, but its role may be much less than 10% of the total compensation of Mg. On the other hand, positron measurements are only sensitive to the neutral V_N-Mg_{Ga} pairs, which may represent only a fraction of all V_N-related defects.

To obtain information on the compensation level of Mg by the vacancy cluster, we assume that the vacancy cluster is decorated by Mg impurities as demonstrated by the TEM results for pyramidal defects. The cluster concentration is obtained from the positron experiments (Table II), and we approximate the maximum passivation effect by assuming that the internal surface of the vacancy cluster is totally covered by Mg atoms. As a result one can deduce that one cluster with a radius of $r=5$ Å can bind a maximum of 100 Mg atoms, which leads to the compensation level of 4.5×10^{17} cm^{-3}. Hence, the total compensation effect by vacancy defects is less than 10^{18} cm^{-3}, which is only a small fraction of the total Mg concentration. The hydrogen passivation thus seems to be the dominant mechanism, but the vacancy defect may explain the additional electrical deactivation of Mg acceptors.

B. Annealing effects

1. Annealing of the vacancy clusters

The results presented here show that the vacancy cluster of about 60 atoms is replaced by smaller clusters during the thermal annealing process. The vacancy cluster consists of vacancies in both sublattices, and the dissociation is a matter of binding energy and the diffusion barrier of the individual monovacancy. According to theory and experimental results,[5,6] the migration barriers of vacancy defects are 3.96, 2.65, and 1.9 eV for V_N^{1+}, V_N^{3+}, and V_{Ga}^{3-}, respectively. The vacancy cluster may thus recover in the following way. At high temperature the cluster dissociates into monovacancies, which diffuse rapidly in the material. The diffusion of monovacancies is slowed down by encountering a vacancy in the opposite sublattice, leading to the formation of smaller vacancy clusters either at the annealing temperature or during cooling down process.

The activation energy of cluster dissociation can be roughly estimated. We use the expression of $N = \omega t e^{-E_A/k_bT}$, where N is the number of jumps of an individual defect in a given lattice, t is the annealing time, and T is the temperature. A prefactor value of $\omega = 1 \times 10^{13}$ s^{-1} is typical for the jump frequency. In order to dissociate a cluster the required number of jumps could be between 1 and 100. In the case of

RTA ($t \approx 100$ s) at 1000 °C we have $E_A = 3.3$–3.8 eV. This value is larger than the theoretical and experimental values for the migration of V_N^{3+}(2.6 eV) and V_{Ga}(1.8 eV). Assuming these migrating species, we estimate the binding energy of the vacancy cluster on the order of 1–2 eV.

The PL spectra of samples with high concentration of Mg acceptors show typically, after thermal annealing, emission bands with peaks in the spectral region between 2.7 and 2.9 eV.[12] This coincides with the appearance of Ga-vacancy-related small clusters formed after the thermal-annealing-induced dissociation of the larger clusters. The observed vacancy clusters are positron traps in both the neutral and the negative charge states. Associating these defects with the 2.7–2.9 eV emission bands is attractive, but a detailed PL study is necessary to establish this identification.

2. Annealing of the V_N-Mg_{Ga} pair

Pairs of N vacancy and Mg dopants are observed here as well as in our previous work.[10] In the present experiments no evidence of V_N-Mg_{Ga} defects is observed after annealing, and our previous results indicate that the concentration of these pairs decreases with annealing between 500 and 800 °C. Since these defects are not observed in MBE samples, which do not require postgrowth thermal annealing to activate the Mg acceptors, we infer that the V_N-Mg_{Ga} complexes are stable in semi-insulating GaN but unstable in p-type materials. During annealing GaN is converted to p type, mainly by the removal of the passivating hydrogen and by the dissociation of the V_N-Mg_{Ga} pairs and migration of V_N. We estimate the migration barrier of V_N as 2.5(3) eV,[10] which is close to the calculated value of V_N^{3+}.[5,6] In fact, the calculations explain the different stabilities of V_N-Mg_{Ga} complexes in p-type and semi-insulating GaN, since the large migration barrier of V_N^{1+} of 3.96 eV makes the V_N-Mg_{Ga} complex very stable when the Fermi level is at midgap.

Recently Wright and Mattsson[6] have calculated the migration barriers of V_N-related defects, with similar results to those found by Limpijumnong and Van de Walle.[5] Wright and Mattsson further analyzed our positron annihilation experiments.[10] According to their theory, the V_N left from the dissociating V_N-Mg_{Ga} complex is able to migrate to the surface during 800 °C annealing. A diffusion length of about 6 Å was estimated for V_N during 500 °C annealing. This is in good agreement with our results at this annealing temperature, where a clear decrease of V_N-Mg_{Ga} concentration was observed.[10] Notice that a small diffusion length of 6 Å is enough to remove the positron trapping at the V_N-Mg_{Ga} complex, since the isolated V_N^{3+} or V_N^{1+} cannot be observed by positron annihilation spectroscopy due to Coulomb repulsion. Furthermore, reduced positron trapping at V_N-Mg_{Ga} pairs is still observed in annealed (500–800 °C) samples,[10]

which already show p-type conductivity [$p = (3-10) \times 10^{16}$ cm^{-3}]. This implies that (i) some of the V_N-Mg_{Ga} complexes survive the annealing, and (ii) at least a fraction of the V_N-Mg_{Ga} complexes remain in the neutral charge state even in p-type GaN, since they are observed as positron traps.

The work of Lee *et al.* and of Wright and Mattsson points out the hydrogen decoration of V_N-related complexes such as V_N-Mg_{Ga} (Ref. 6) or V_N-Mg_i.[40] While we agree that such complexing may be possible, we do not think that V_N-Mg_{Ga}-H complexes would trap positrons, since the presence of H decreases the open volume and increases the positive charge of the complex. The removal of H from V_N-Mg_{Ga}-H complexes during annealing would increase the positron trapping at V_N defects, which contradicts our experimental observation. Therefore, we believe that the V_N-Mg_{Ga} defects observed in the present or in the previous work[10] are unlikely to be decorated with hydrogen.

V. CONCLUSION

We have studied Mg-doped GaN films with positron annihilation spectroscopy to find out the effect of Mg doping, Si codoping, and thermal annealing on open volume defects. Vacancy-related defects are observed only for Mg doping levels of about 10^{19} cm^{-3}. Studies of unannealed GaN:Mg sample resulted in the detection of two vacancy defects; one with a positron lifetime of 180 ps and the other with a lifetime of 435 ps. They are identified as V_N-Mg_{Ga} and vacancy clusters, respectively.

The vacancy clusters have an inhomogeneous depth profile in the unannealed GaN:Mg, typically a lower concentration down to 100 nm from the surface. The concentration of V_N-Mg_{Ga} changes less throughout the layer. Annealing dissociates V_N-Mg_{Ga} pairs as well as the vacancy clusters, which leads to a uniform vacancy distribution through the film. The vacancy defect formed by the dissociated vacancy clusters is identified as a Ga-vacancy-related smaller cluster. The samples codoped with Si donors show similar behavior to that observed in the samples doped only with Mg.

Before annealing the concentration of V_N-Mg_{Ga} is estimated of $(2-3) \times 10^{17}$ cm^{-3} while the vacancy cluster concentration varies in the range $(0.5-5) \times 10^{15}$ cm^{-3}, with a region of lower concentration just below the surface. These defects compensate Mg acceptors in GaN. The quantitative estimates presented here, however, suggest that the hydrogen passivation of Mg is the dominant deactivation mechanism.

ACKNOWLEDGMENT

*On leave from KFKI Central Research Institute for Nuclear and Particle Physics, H-1525 Budapest P.O.B. 49, Hungary.

[1] S. Nakamura, T. Mukai, M. Senoh, and N. Iwasa, Jpn. J. Appl. Phys., Part 2 **31**, L139 (1992).

[2] H. Amano, M. Kito, K. Hiramatsu, and I. Akasaki, Jpn. J. Appl. Phys., Part 2 **28**, L2112 (1989).

[3] U. Kaufmann, M. Kunzer, M. Maier, H. Obloh, A. Ramakrishnan, B. Santic, and P. Schlotter, Appl. Phys. Lett. **72**, 1326 (1998).

[4] I. Gorczyca, A. Svane, and N. E. Christensen, Phys. Rev. B **61**, 7494 (2000).

[5] S. Limpijumnong and C. G. Van de Walle, Phys. Rev. B **69**, 035207 (2004).

[6] A. F. Wright and T. R. Mattsson, J. Appl. Phys. **96**, 2015 (2004).

[7] Z. Liliental-Weber, M. Benamara, W. Swider, J. Washburn, I. Grzegory, and S. Porowski, Phys. Rev. Lett. **83**, 2370 (1999).

[8] Z. Liliental-Weber, M. Benamara, W. Swider, J. Washburn, I. Grzegory, S. Porowski, D. J. H. Lambert, C. J. Eiting, and R. D. Dupuis, Appl. Phys. Lett. **75**, 4159 (1999).

[9] R. Krause-Rehberg and H. S. Leipner, *Positron Annihilation in Semiconductors* (Springer-Verlag, Berlin, 1999).

[10] S. Hautakangas, J. Oila, M. Alatalo, K. Saarinen, L. Liszkay, D. Seghier, and H. P. Gislason, Phys. Rev. Lett. **90**, 137402 (2003).

[11] Jeremy Moxom, Jun Xu, R. Suzuki, T. Ohdaira, George Brandes, and Jeffrey S. Flynn, J. Appl. Phys. **92**, 1898 (2002).

[12] E. R. Glaser, W. E. Carlos, G. C. B. Braga, J. A. Freitas, Jr., W. J. Moore, B. V. Shanabrook, R. L. Henry, A. E. Wickenden, D. D. Koleske, H. Obloh, P. Kozodoy, S. P. DenBaars, and U. K. Mishra, Phys. Rev. B **65**, 085312 (2002).

[13] P. Laukkanen, S. Lehkonen, P. Uusimaa, M. Pessa, J. Oila, S. Hautakangas, K. Saarinen, J. Likonen, and J. Keränen, J. Appl. Phys. **92**, 786 (2002).

[14] M. A. Reshchikov, G.-C. Yi, and B. W. Wessels, Phys. Rev. B **59**, 13176 (1999).

[15] H. Teisseyre, T. Suski, P. Perlin, I. Grzegory, M. Leszczynski, M. Bockowski, S. Porowski, J. A. Freitas, Jr., R. L. Henry, A. E. Wickenden, and D. D. Koleske, Phys. Rev. B **62**, 10151 (2000).

[16] K. Saarinen, P. Hautojärvi, and C. Corbel, *Identification of Defects in Semiconductors* (Academic, New York, 1998).

[17] J. Oila, V. Ranki, J. Kivioja, K. Saarinen, P. Hautojärvi, J. Likonen, J. M. Baranowski, K. Pakula, T. Suski, M. Leszczynski, and I. Grzegory, Phys. Rev. B **63**, 045205 (2001).

[18] K. Saarinen, J. Nissilä, P. Hautojärvi, J. Likonen, T. Suski, I. Grzegory, B. Lucznik, and S. Porowski, Appl. Phys. Lett. **75**, 2441 (1999).

[19] J. Oila, K. Saarinen, A. E. Wickenden, D. D. Koleske, R. L. Henry, and M. E. Twigg, Appl. Phys. Lett. **82**, 1021 (2003).

[20] K. Saarinen, T. Laine, S. Kuisma, J. Nissilä, P. Hautojärvi, L. Dobrzynski, J. M. Baranowski, K. Pakula, R. Stepniewski, M. Wojdak, A. Wysmolek, T. Suski, M. Leszczynski, I. Grzegory, and S. Porowski, Phys. Rev. Lett. **79**, 3030 (1997).

[21] E. Calleja, M. A. Sánchez-García, D. Basak, F. J. Sánchez, F. Calle, P. Youinou, E. Muñoz, J. J. Serano, J. M. Blanco, C. Villar, T. Laine, J. Oila, K. Saarinen, P. Hautojärvi, C. H. Molloy, D. J. Somerford, and I. Harrison, Phys. Rev. B **58**, 1550 (1998).

[22] These calculations are based on the generalized gradient approximation for positron-electron correlation.

[23] R. M. Nieminen, J. Laakkonen, P. Hautojärvi, and A. Vehanen, Phys. Rev. B **19**, 1397 (1979).

[24] T. E. M. Staab, M. Haugk, T. Frauenheim, and H. S. Leipner, Phys. Rev. Lett. **83**, 5519 (1999).

[25] M. J. Puska and R. M. Nieminen, J. Phys. F: Met. Phys. **13**, 333 (1983).

[26] M. J. Puska and R. M. Nieminen, Rev. Mod. Phys. **66**, 841 (1994).

[27] E. Boronski and R. M. Nieminen, Phys. Rev. B **34**, 3820 (1986).

[28] W. Brandt and J. Reinheimer, Phys. Lett. **35A**, 109 (1971).

[29] R. Krause-Rehberg, H. S. Leipner, A. Kupsch, A. Polity, and Th. Drost, Phys. Rev. B **49**, 2385 (1994).

[30] R. Krause-Rehberg, M. Brohl, H. S. Leipner, Th. Drost, A. Polity, U. Beyer, and H. Alexander, Phys. Rev. B **47**, 13266 (1993).

[31] M. J. Puska, C. Corbel, and R. M. Nieminen, Phys. Rev. B **41**, 9980 (1990).

[32] W. Götz, N. M. Johnson, D. P. Bour, M. D. McCluskey, and E. E. Haller, Appl. Phys. Lett. **69**, 3725 (1996).

[33] B. Clerjaud, D. Côte, A. Lebkiri, C. Naud, J. M. Baranowski, K. Pakula, D. Wasik, and T. Suski, Phys. Rev. B **61**, 8238 (2000).

[34] S. Limpijumnong, J. E. Northrup, and C. G. Van de Walle, Phys. Rev. B **68**, 075206 (2003).

[35] Z. Liliental-Weber, Y. Chen, S. Ruvimov, and J. Washburn, Phys. Rev. Lett. **79**, 2835 (1997).

[36] Z. Liliental-Weber, T. Tomaszewicz, D. Zakharov, J. Jasinski, and M. A. O'Keefe, Phys. Rev. Lett. **93**, 206102 (2004).

[37] Z. Liliental-Weber, T. Tomaszewicz, D. Zakharov, J. Jasinski, M. A. O'Keefe, S. Hautakangas, A. Laakso, and K. Saarinen, in MRS Symposia Proceedings No. 798, edited by Hock Min Ng, Michael Wraback, Kazumasa Hiramatsu, and Nicolas Grandjean (Materials Research Society, Pittsburgh, 2004), p. Y9.7.

[38] B. Santic, Semicond. Sci. Technol. **18**, 219 (2003).

[39] We use the basic approach for the approximation of the Fermi level in a nondegenerate semiconductor material

$$[N_a - N_d] = N_v e^{-(E_F - E_V)/k_b T},$$

where $N_v = 2(2\pi m_h k_b T/\hbar^2)$. The concentration of activated acceptors is $[N_a^-] = [\text{Mg}]f(E_a)$, where $f(E_a)$ is the Fermi function.

[40] S.-G. Lee and K. J. Chang, Semicond. Sci. Technol. **14**, 138 (1999).